# Gas sensing (RuPc)₂ thin films: Electrical response to NO₂ gas and morphological changes induced by external moisture

Amanda Generosi [a], Barbara Paci [a,*], Valerio Rossi Albertini [a], Renato Generosi [a], Anna Maria Paoletti [b], Gianna Pennesi [b], Gentilina Rossi [b], Marco Fosca [c], Ruggero Caminiti [c]

[a] Istituto di Struttura della Materia-Area di Ricerca di Tor Vergata, Via del Fosso del Cavaliere 100, 00133 Roma, Italy
[b] Istituto di Struttura della Materia-Area di Ricerca di Montelibretti, Via Salaria Km. 29.5, CP10 Monterotondo Stazione, Roma, Italy
[c] Dipartimento di Chimica, Università "La Sapienza" di Roma e sezione INFM, P.le A. Moro 5, 00185 Roma, Italy

### ABSTRACT

The morphological changes induced in (RuPc)₂ gas sensing thin films by hydration and de-hydration processes were investigated. Prior to this study a preliminary characterization was performed by conductivity measurements upon exposure to NO₂ gas fluxes, to verify the electrical sensing response of the films. This response was correlated to the bulk morphological modification of the films. Subsequently, the effect of external moisture on the morphological stability of the films was addressed. This morphological characterization of the films was performed by using the energy dispersive X-ray reflectivity (EDXR) and atomic force microscopy (AFM) techniques, both *ex situ* and *in situ*, i.e. under operating conditions, during exposure of these films to 100% of relative humidity. The measurements allowed an accurate observation of both the surface morphology (i.e. its roughness obtained independently by EDXR and AFM). Moreover bulk evolution of the films was obtained by *in situ* EDXR and the morphological changes allowed to retrieve information on the water uptake dynamics. Moreover, the reversibility of the water/film interaction was studied and correlated to the sensing properties of the (RuPc)₂.

© 2008 Elsevier B.V. All rights reserved.

## 1. Introduction

Metallophythalocyanines (MPcs) [1] are multipurpose synthetic electroactive materials with peculiar electronic and structural characteristics, which show semiconducting and non-linear optical properties. In particular, the electrical properties of MPcs are modulated upon exposure to gases such as NO₂ or ammonia [2,3], and this phenomenon has led to an interest in developing gas detectors using Pc derivatives as the chemically sensitive component [4,5]. Recently, it has been proved that the chemical nature of the sensitive layer is not the only feature to take into account, in order to improve the sensor performances [6]. Indeed, morphology of the active layer (thickness and roughness) strongly affects the response/recovery times and the behaviour of MPcs at room temperature as well as at high temperatures [7–9]. Recent studies demonstrated that suitable thermal treatments are able to stabilize the morphology of these materials [10]. This stabilization results in an improvement of response time, of recovery rate and of the behaviour at room temperature. However, this is not the case for properties like selectivity and sensitivity that, even after thermal treatments, still need to be improved. Indeed, they may be affected by external agents, such as chemical interaction occurring between MPcs and molecules present in the environment together with the chemical agents to be detected. In this context it is important to clarify the effect on the sensor performances of water vapour, always present, to some extent, in the ambient atmospheres where the sensors operate [11]. In this work, the morphology changes induced by humidity and the effect on the sensing capability of a specific MPc are investigated. A (RuPc)₂ thin film, which exhibited an enhancement of its sensing properties as a consequence of thermal-induced morphological stabilization, was chosen as a reference system [12,13]. The evolution of the film morphological parameters during the interaction of water molecules with the Pc films [11,14] was followed by means of both *in situ* time-resolved energy dispersive X-ray reflectivity (EDXR) and atomic force microscopy (AFM).

## 2. Experimental

X-ray reflectivity is highly sensitive to electron density gradients, regardless of the structure of the system investigated (crystalline, amorphous, etc.). Moreover, it is also one of the few methods that enable one to calculate the roughness of both the free surfaces and the interface(s) with great accuracy, together

with the thickness of various layers that compose a stratified specimen [15,16]. This experimental technique was used in the energy dispersive mode, which is particularly advantageous when *in situ* time-resolved measurements are performed. A reflectivity measurement consists of collecting the reflected intensity as a function of the scattering parameter, $q = 4\pi \sin\alpha/\lambda = KE \sin\alpha$ ($K = 1.014$ is a constant value, $E$ the radiation energy and $\alpha$ is half the scattering angle), which depends on the radiation energy and the scattering angle. It follows that two methods are available for carrying out the $q$ scan and reflected intensity profile as a function of $q$ [17]. The first is to use a monochromatic beam (fixed energy), for instance a fluorescence line produced by a laboratory X-ray tube, and to make an angular scan, called angular dispersive (AD) mode. The second consists of utilizing a continuum spectrum radiation, for example the "bremsstrahlung" (braking radiation) of the same X-ray tube (often called *white beam* in analogy with visible light), and to maintain the scattering angle fixed during the reflectivity pattern collection, often reported as the energy dispersive (ED) mode [18]. The main advantage is that the experimental geometry remains unchanged during data collection, which greatly simplifies *in situ* time-resolved studies [19,20].

The reflectometry measurements were performed by a non-commercial energy dispersive machine [17] that, from a geometrical point of view, is similar to a conventional angular dispersive one, the main differences being the absence of monochromator and the use of an X-ray spectrometer as a detector.

An ordinary X-ray W anode tube was used as the radiation source. The non-monochromatized radiation is collimated by an adjustable slit and directed onto the sample. After being reflected, it is collimated again by a further two slits and, finally, acquired by the energy sensitive detector.

The X-ray detector is an EG&G solid-state device (SSD) whose sensitive part is a semiconducting high-purity germanium single crystal, capable of determining the energy of each incoming photon.

Especially designed environmental chambers were mounted on both the reflectometer and the AFM. They allow the relative humidity (RH) to be maintained at a stable level or, alternatively, to flux drying inert gases ($N_2$) onto the samples.

The $(RuPc)_2$ films were deposited by sublimation of a $(RuPc)_2$ powder on a Si (1 1 1) wafer in a vacuum chamber ($10^{-5}$ mbar to $10^{-6}$ mbar) [21]. The powder is characterized by a crystalline nature and by the contamination of pyridine molecules which are entrapped into the lattice. The powder holder is heated by a heating resistor and a shutter is kept closed until a 300-°C temperature is reached, to protect the Si substrate to avoid the deposition of undesired contaminating molecules. Indeed at this temperature the sublimation of the pyridines destabilizes the crystalline structure of the $(RuPc)_2$ powder, this process being responsible for the amorphous nature of the deposited film [22,23]. When the temperature reaches 320 °C the shutter can be removed and the deposition begins. The temperature progressively grows, and consequently the deposition rate, up to a limit of 500 °C at which the $(RuPc)_2$ powder decomposes. The growth is monitored by an Edwards FTM5 quartz crystal balance, by measuring the change in its resonance frequency consequent to its exposure to the $(RuPc)_2$ flux during the film deposition. When the desired thickness is reached, the shutter is closed and finally when the deposition chamber is cooled down to 30–35 °C the pressure is turned back to the atmosphere value.

## 3. Results and discussion

At first, as a preliminary sensitivity test, time-resolved conductivity measurements were performed upon $(RuPc)_2$ thin films exposed to $NO_2$ gas fluxes. Indeed, in previous works it was proven that the diffusive bulk interaction between the phthalocyanine π-electrons and the oxidizing gas modulated the device response to $NO_2$ on a morphological basis [7–10]. Now confirmation of an electrical response is required.

The devices were produced by sublimating the $(RuPc)_2$ powder onto interdigitated Au electrodes under vacuum. No post-deposition annealing was performed on the films since this method stabilizes the structure and morphology of the samples, altering their natural behaviour towards gas molecules, which is not the aim of this work. Two-contact electrical measurement was performed by applying a 0.8-V voltage across the electrodes and collecting the current intensity values as a function of $NO_2$ exposure time.

The test measurements were performed by maintaining a 20 nmol/s $NO_2$ (50 ppm) in 180 nmol/s $N_2$ gas flux and in Fig. 1 the electrical response of a 65-nm thick $(RuPc)_2$ film is plotted as an example. In the inset of Fig. 1, the *ex situ* reflectivity patterns collected on the film before and after exposure to the $NO_2$ gas flux are shown. Indeed, the variation of the oscillation frequency (enhanced by the arrows connecting the third minima) and of their damping is visible. This modification is due to the change of the film thickness ($d$) and roughness ($s$), respectively, as a consequence of the film–gas interaction [7–10]. The Parratt fit [15] of the reflectivity patterns allowed to deduce the initial and final thickness and roughness of the film: $\Delta d = 3.5(5)$ nm and $\Delta s = 1.00(5)$ nm. The overall conductivity change proved to be easily detectable, the characteristic response times being comparable to those observed in other Pc systems which have been patented as $NO_2$ sensors [24]. Moreover the electrical response was found to be related to a morphological variation of the film, as observed in other phthalocyanine systems (TiPc devices) [25]. It follows that morphology is an important parameter to control and, therefore, the further investigations in the present study focused on the morphological response of the film.

In the following, AFM was used *in situ*, in combination with *ex situ* EDXR measurements, in order to follow the real-time structural changes induced on a $(RuPc)_2$ gas sensing film by the presence of ambient moisture which has been proved to be one of the most interfering factors for the MPc sensing systems [11].

*Ex situ* measurements, performed upon a $(RuPc)_2$ film before and after exposure to a 100% RH atmosphere are reported in Fig. 2. The comparison between the reflection pattern of the as-deposited sample (upper curve), and the pattern collected after the film was exposed for 12 h to an atmosphere, at the dew point (lower curve)
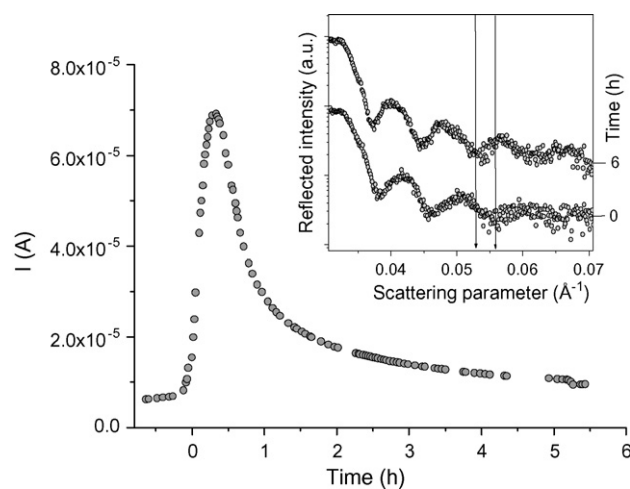


**Fig. 1.** Electrical conductivity variation of a $(RuPc)_2$ device when exposed to a 50-ppm $NO_2$ gas flux in 180 nmol/s of $N_2$ driving gas. In the inset, the reflectivity profiles, collected before (lower curve) and after (upper curve) the exposure to the pollutant, clearly show that a morphological rearrangement of the film has occurred (shift of the oscillations).
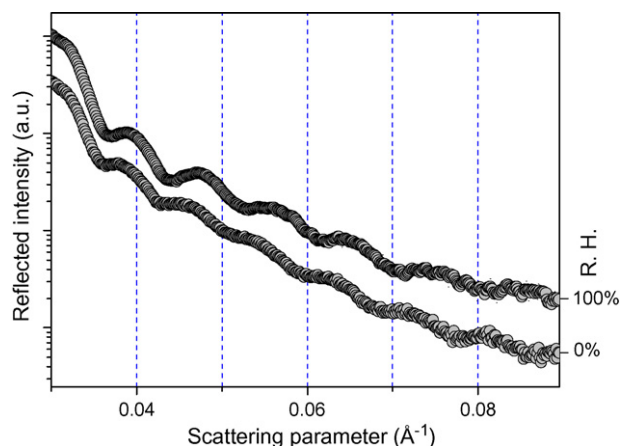
**Fig. 2.** (a) Reflectivity patterns collected upon a 50-nm nominally thick (RuPc)$_2$ film before (upper spectrum) and after (lower spectrum) a 12-h exposure to a 100% RH atmosphere. The shift of oscillations maxima toward lower $q$-values and their damping reveal that morphological changes have occurred.

reveals that morphological changes occurred. In particular, by a quantitative Parratt analysis of the patterns [15], the initial and final thickness ($d$) and roughness ($s$) result in the values of $d_i = 42.5(5)$ nm and $d_f = 46.3(5)$ nm, $s_i = 0.40(5)$ nm and $s_f = 1.00(5)$ nm. The interaction involves both the film bulk and its surface: indeed a relevant increase of the total thickness, consistent with a diffusion process, is observable and the film roughness is strongly affected. Indeed the (RuPc)$_2$ films are known to absorb/desorb gas molecules with a "breathing-like mechanism", the lattice swelling being approximately 5% of the initial film thickness. In this case, however, the swelling appears to be much more consistent (ca. 10%), indicating that the water molecules widely diffuse into the lattice maybe affecting the mechanical recovery capability of the lattice.

Subsequently, in order to monitor the real-time evolution of the interaction between the (RuPc)$_2$ film and the H$_2$O molecules, time-resolved AFM images (3 μm × 3 μm) were collected from the

same area under saturated humidity conditions. The experimental parameters were set in order to acquire an image every hour. A sequence of such images was collected to sample the same area and thus observe the surface changes in real time.

In Fig. 3, the initial image, collected on the as-deposited film, is compared with those obtained after the (RuPc)$_2$ was kept for 1–5 h (Fig. 3b–f) in a 100% RH atmosphere. A black circle is drawn on a clearly visible granular domain that can be taken as a reference point. In this way, it is shown that no shift of the images occurs and the same portion of the surface is sampled in each micrograph.

Focusing on this zone, which represents a raised structure on the (otherwise almost flat) surface, the effect of the water vapour–film interaction is clarified. The other parts of the surface gradually swell until the whole film is covered by structures similar to that in the circle.

The structure in the circle was identified as a defect and its characteristic dimensions (RMS-mean) strongly differ from the parameters corresponding to the as-deposited film. However, the film surface evolves over time and its characteristic dimensions grow similar to that of the defected zone. Moreover, an ordered texture appears, consisting of parallel stripes (average dimensions: 0.25-μm wide × 1.5-μm long × 30-nm high) that arise during the water vapour uptake. Analysing highlights of the image sequence, it is clear that the texturing is due to the swelling of the initially smooth surface, as will be discussed later in the text. This observation suggests that the water molecules diffuse into the film lattice, the surface growing effect not being related to random surface adsorption, but to the swallowing of the under laying (RuPc)$_2$ bulk. However, due to the 100% RH, a dynamic equilibrium occurring onto the surface must be taken into account, even when the (RuPc)$_2$/H$_2$O interaction saturates, as testified by the good overlapping of the image collected after 5 h and the one obtained after 12 h appreciated by the naked eye. To extrapolate the accurate time evolution of the surface roughness (Rms), the analysis of the AFM images was carried out by calculating the average Rms on the whole image, after correction of the experimental artefacts. The evolution of this parameter as a function of the 100% RH exposure time is shown
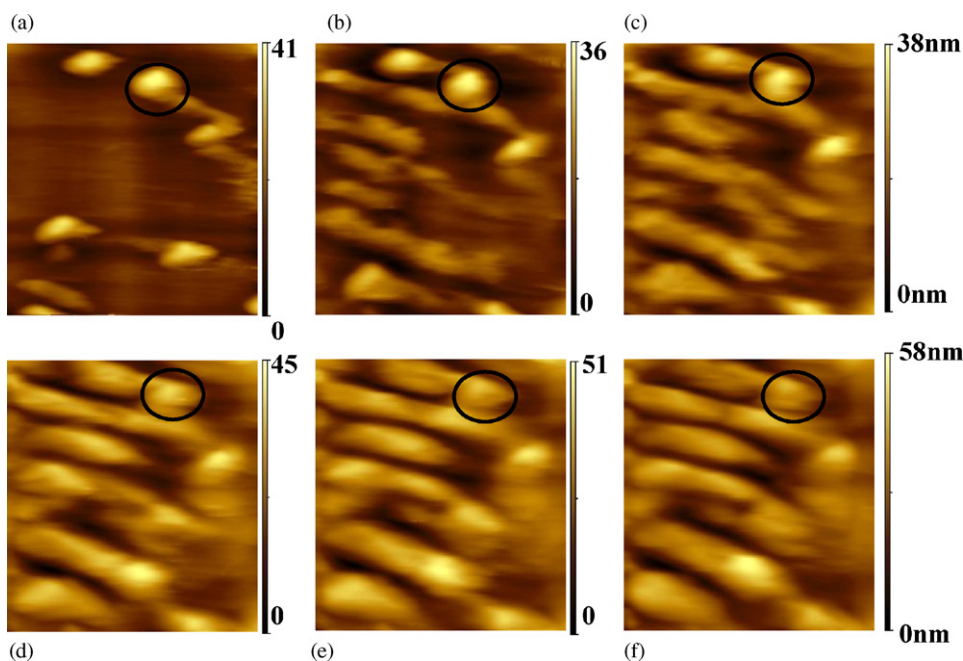


**Fig. 3.** AFM images (3 μm × 3 μm) collected during the exposure of a (RuPc)$_2$ film (the same sample of Fig. 2) to a 100% RH. (a) The as-deposited film micrograph is shown; (b–f) the micrographs after 1 h, 2 h, 3 h, 4 h, and 5 h, respectively. The images (e) and (f) perfectly overlap, indicating the humidity–film interaction is concluded and the film is saturated with water.
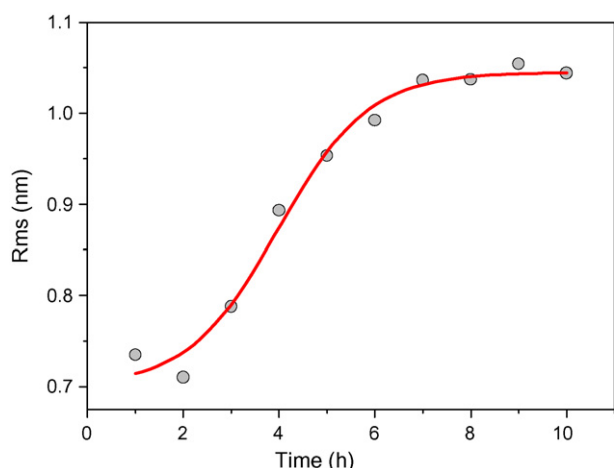
**Fig. 4.** Time evolution of the Rms, as deduced by the quantitative analysis of the AFM images, as a function of exposure time to the 100% RH atmosphere. The continuous line represents the Boltzmann fit of the roughness increase, calculated from these images.

in Fig. 4. As expected the trend is perfectly fitted by a Boltzmann growth, the characteristic time of the process being about 4 h, and the complete saturation actually corresponding to 7 h.

The films were subjected to different processes in order to establish whether the water uptake was a completely reversible process, and to evaluate its interference with the (RuPc)$_2$ gas-sensing capability. At first, a standard cleaning procedure, fluxing N$_2$ gas molecules (200 nmol/s) into the experimental chamber in order to dry the film, was performed: both the (RuPc)$_2$ morphology parameters ($d$ and $s$ measured by EDXR) and the AFM topography remained unchanged. Afterwards the (RuPc)$_2$ film was submitted to a 24-h heating at 50 °C under controlled atmosphere (N$_2$ gas flux, 200 nmol/s), to ensure the desorption of any water molecules without inducing further thermal effects on the film's structure and morphology.

To monitor the morphological changes induced by the thermal treatment, the heating was carried out in a special oven designed for this purpose, which allowed the real-time acquisition of reflectivity patterns. In Fig. 5, the sequence of the spectra collected over 24 h is shown, the time resolution of each acquisition being 15 min. As evidenced by the arrow connecting the minima of the third oscillation, a compression of the fringes occurs during the first hours of the thermal treatment, and subsequently the patterns tend to an asymptotic shape corresponding to the new steady condition. By the Parratt fitting of each pattern, the thickness and roughness variations were deduced as a function of time (see Fig. 6). Both parameters show an exponential decay, the characteristic times being $\tau_d = (0.50 \pm 0.25)$ h and $\tau_\sigma = (0.80 \pm 0.25)$ h, respectively. The average thickness and roughness loss corresponds to $\Delta d = 1.00(5)$ nm and $\Delta \sigma = 0.15(5)$ nm. These values are consistent with partial desorption of the water molecules confined into the first film layers from the surface.

Indeed, new AFM images collected after the thermal treatment are perfectly comparable to the previous ones, although the explored zone on the surface is not the same as Fig. 2. Since the film deposition is extremely uniform, this is an evidence that the surface has turned back to its original shape. In Fig. 7, 2 μm × 2 μm images collected before water uptake (a), after saturation (b) and after thermal treatment (c) are plotted in the form of 3D maps. The first and last images represent a clean, finely textured surface. This is a further evidence that the surface desorption has taken place during the 50 °C thermal treatment. Moreover, it is also clearly visible that the water uptake has been mainly a bulk effect, inducing the swelling of
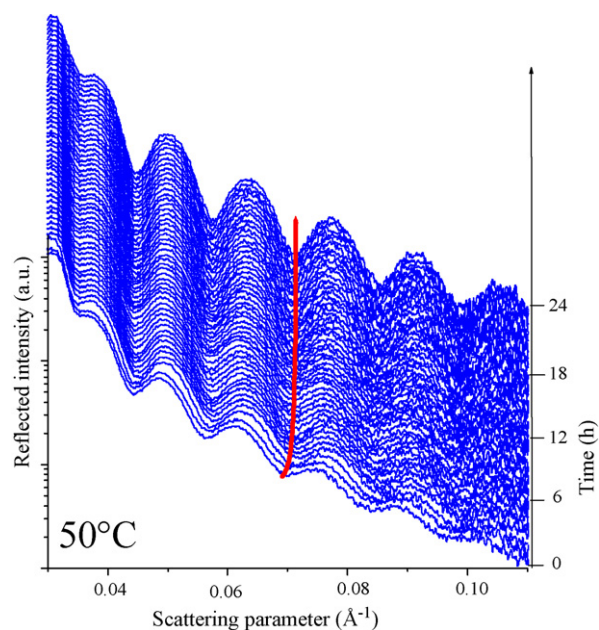


**Fig. 5.** Sequence of reflectivity patterns, collected upon the (RuPc)$_2$ film, as a function of the scattering parameter $q$ and of time, during a thermal treatment at 50 °C. The arrow connecting the fourth minima of the oscillations evidences the morphological changes occurring.

the underlayer film lattice. Indeed, the parallel stripes arising after saturation (Fig. 7b), perfectly correspond to the coalescence of the initial granular structure retaining the lamellar preferential growth that is evidenced by an arrow in Fig. 7.

These considerations further support the hypothesis of water bulk diffusion and of consequent swelling of the film structure.

In order to achieve the complete desorption of water molecules from the (RuPc)$_2$ bulk, the same procedure which is usually used to reset the material after a gas sensing cycle, was applied, to guarantee that no modifications may be induced by the external physical treatment.

The sample was submitted to two consecutive thermal treatments at 100 °C and 130 °C, respectively under controlled atmosphere (24 h each) collecting EDXR spectra (15 min each) during the whole procedure, as shown by the sequence of patterns
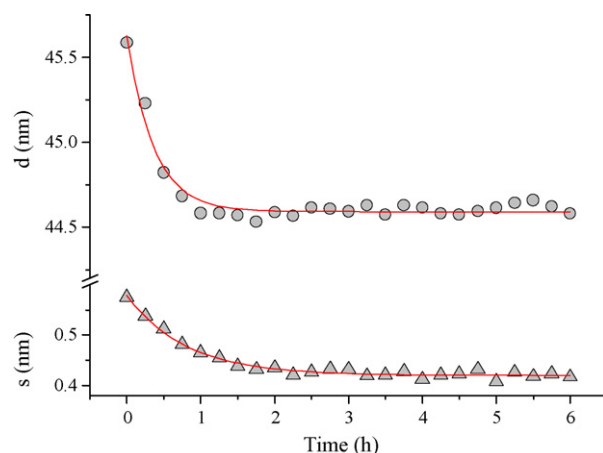


**Fig. 6.** Time evolution of the morphological parameters thickness ($d$) and roughness ($s$) as obtained by the accurate fitting of each reflectivity spectrum shown in Fig. 5. The continuous lines are the exponential decays fitting the morphological evolution of the (RuPc)$_2$ thin film during hydration.
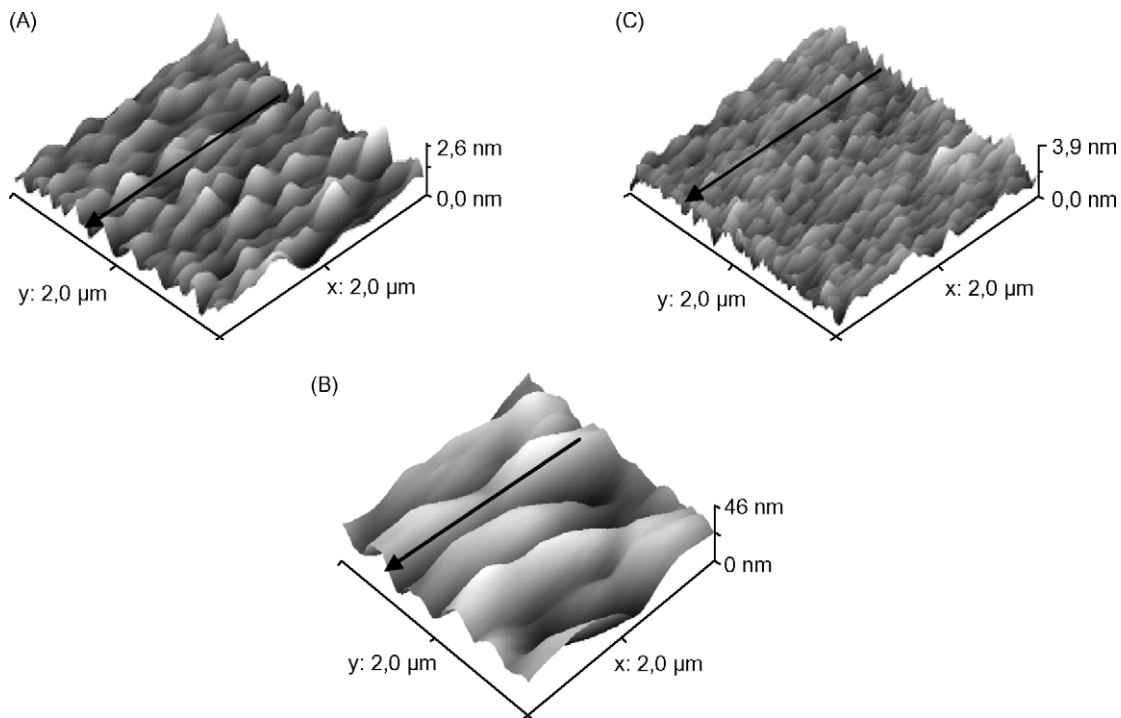
**Fig. 7.** AFM images collected upon (A) the as-deposited (RuPc)$_2$ film, (B) after its exposure to 100% RH and (C) after its exposure to 100% RH and a subsequent thermal treatment at 50 °C for 24 h. In (C), a substantial decrease of the film roughness with respect to (B) can be noticed.

plotted in Fig. 8. These temperatures were chosen since 100 °C is the H$_2$O critical evaporation point and 130 °C has proven to be a critical temperature for the (RuPc)$_2$ inducing structural rearrangements [10].

As indicated by the arrow connecting the second minimum of the first oscillation (moving towards higher $q$-values at first and to lower $q$-values subsequently), the film morphology changes



**Fig. 8.** Sequence of reflectivity patterns, collected upon the (RuPc)$_2$ film, as a function of the scattering parameter $q$ and of time, during two subsequent thermal treatments at 100 °C and 130 °C, respectively. The arrow connecting the first minima of the oscillations evidences the morphological changes occurring during the thermal treatment.

dramatically during the first 4 h of the thermal treatment. This qualitative evolution was quantified (Fig. 9) by the accurate Parratt fitting of each spectra, deducing the thickness and roughness time evolution during the isothermal treatments. The changes can be summarized as follows:

(1) A sigmoidal thickness increase ($\Delta d = 3.50(5)$ nm), with a characteristic time of $\tau(d)'_{100°} = (0.90 \pm 0.25)$ h occurs; the roughness remains stable. This indicates that the applied thermal energy is transmitted to the entrapped water molecules, enhancing their mobility and inducing a bulk rearrangement resulting in a thickness increase. The surface is not involved in this bulk process.
(2) Subsequently a thickness and roughness exponential decrease occurs ($\Delta d = 1.00(5)$ nm and $\Delta s = 0.20(5)$ nm)
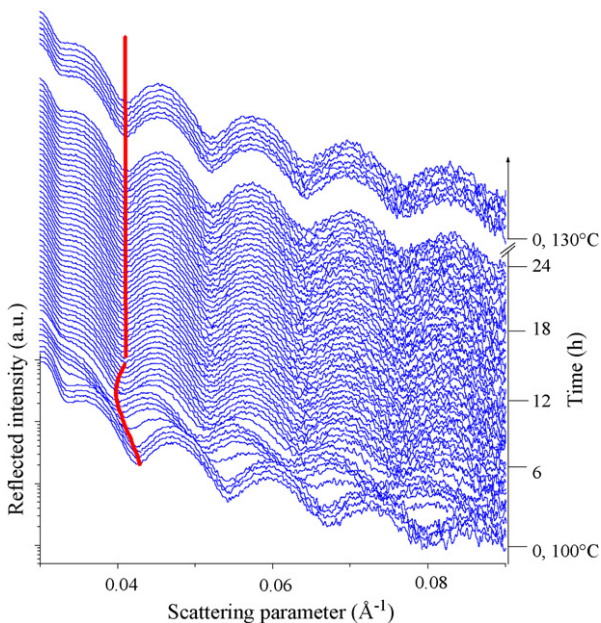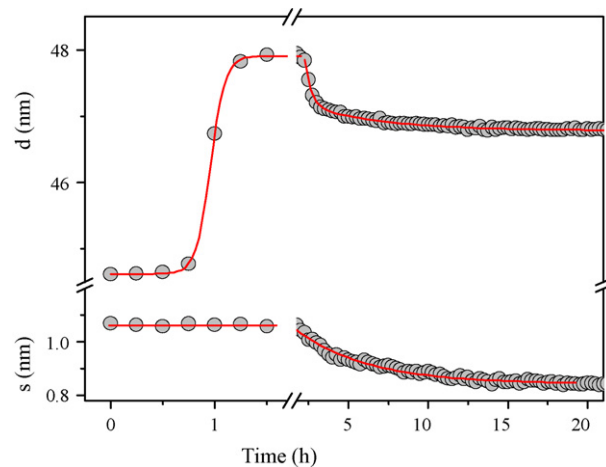


**Fig. 9.** Time evolution of thickness and roughness as obtained by the accurate Parratt fit of each EDXR spectrum shown in Fig. 8.

with a characteristic times of $\tau(d)''_{100°} = (5.00 \pm 0.25)\,h$ and $\tau(s)''_{100°} = (4.75 \pm 0.25)\,h$, respectively. This phenomenon is analogous to the one occurred when the same film was submitted to the 50 °C thermal treatment, despite the time scale is now wider. Indeed, the first layers of the film and its surface are involved (the characteristic times of the $d$, the $\sigma$ evolutions being coincident) and released entrapped water molecules. Due to molecules enhanced mobility and film rearrangement induced by the thermal energy (as described above), a layer of molecules was able to move towards the film surface and to desorb overcoming the film's mechanical surface adhesion.

(3) Finally, saturation of the thickness and roughness parameters occurs, the main values remain constant during the further 100 °C thermal treatment. The saturation remains stable also when the subsequent 130 °C thermal treatment is performed. This indicates that the bulk rearrangement is concluded and that the entrapped water molecules are confined into the bulk, thus not being able to escape from the film lattice any longer. When the temperature is enhanced to 130 °C, which has been proved to be a critical temperature for $(RuPc)_2$ inducing structural stabilizing effects, the film bulk and surface are not influenced, the water molecules still being entrapped into the lattice. This is an hint indicating that the prior water uptake and the subsequent thermal treatments have degraded the $(RuPc)_2$ molecules packing thus inhibiting any further reset of the sensing material.

When the film was at room temperature, the morphological changes due to water uptake still remained, regardless of the samples thermal history, indicating that the process is irreversible.

## 4. Conclusions

In conclusion, *in situ* electrical measurements and *ex situ* EDXR experiments were performed on $(RuPc)_2$ film-based devices, to verify the film sensor properties and the associated morphological variations. Subsequently, the work focused on an important aspect of the application of gas sensors: the problem of interfering agents (namely $H_2O$). The approach used was based on the study of the morphological properties of the system, by EDXR and AFM measurements. The result demonstrated the sensitivity of $(RuPc)_2$ films towards water molecules, thus inhibiting its potential as sensing material under conditions of high relative humidity. The $(RuPc)_2/H_2O$ interaction was investigated to provide information about the mechanism of water uptake, resulting in an irreversible bulk diffusion. Indeed, contrary to what happens when the gas sensing mechanism is activated, the water uptake process corrupts the mechanical properties of the film matrix, thus inhibiting its sensing potential. Finally, different thermal treatments were applied to the system in an attempt to find a recycling reset procedure, but once more the $(RuPc)_2/H_2O$ system proved to be irreversibly corrupted. Indeed, the film structure and morphology were deteriorated by the water uptake and were not subsequently regained.

## References

[1] F.H. Moser, A.L. Thomas, The Phthalocynines, vols. 1–2, C.R.S. Press, Bocaaton, FL, 1983.

[2] C. Hamann, A. Mrwa, M. Müller, W. Göpel, M. Rager, Lead phtalocyanine thin films for $NO_2$ sensors, Sens. Actuators B 4 (1991) 73–78.

[3] J. Souto, R. De Aroca, J.A. Saja, Gas adsorption and electrical conductivity of Langmuir–Blodgett films of terbium bisphthalocyanine, J. Phys. Chem. 98 (1994) 8998–9001.

[4] A. Capobianchi, A.M. Paoletti, G. Pennesi, G. Rossi, S. Panero, Electrochromism in sandwich-type diphthalocyanines: electrochemical and spectroscopic behaviour of bis(phthalocyaninato)titanium(IV) $(Ti(Pc)_2)$ film, Synth. Met. 75 (1995) 37–42.

[5] F. Baldini, A. Capobianchi, A. Falai, G. Pennesi, A new sandwich-type diphthalocyanine as a potential optical transducer for $NO_2$ detection, Sens. Actuators B: Chem. 51 (1998) 176–180.

[6] A. de Haan, A. Decroly, Electrical resistance of copper phthalocyanine films as influenced by substrates, electrodes and physical features of the films, Sens. Actuators B 30 (1996) 143–150.

[7] A. Generosi, B. Paci, V. Rossi Albertini, P. Perfetti, G. Rossi, A.M. Paoletti, G. Pennesi, R. Caminiti, Morphological variations as non-standard test parameters to determine the sensitivity and the detection limit of gas sensing films: an application to ruthenium phthalocyanine, Appl. Phys. Lett. 88 (2006) 104106–104108.

[8] A. Generosi, B. Paci, V. Rossi Albertini, P. Perfetti, A.M. Paoletti, G. Pennesi, G. Rossi, R. Caminiti, In situ energy dispersive X-ray reflectometry measurements on plastic solar cells upon working, Appl. Phys. Lett. 87 (2005) 181904–181906.

[9] V. Rossi Albertini, A. Generosi, B. Paci, P. Perfetti, G. Rossi, A. Capobianchi, A.M. Paoletti, R. Caminiti, Time resolved energy dispersive X-ray reflectometry measurements on phthalocyanine gas sensor films upon working, Appl. Phys. Lett. 82 (2003) 3868–3870.

[10] A. Generosi, B. Paci, V. Rossi Albertini, P. Perfetti, A.M. Paoletti, G. Pennesi, G. Rossi, R. Caminiti, Enhancing the gas sensing properties of $(RuPc)_2$ thin films by thermal-induced morphological stabilising effects, J. Phys. Chem. C 111 (2007) 12045–12051.

[11] G. Jarosz, P.D. Quinn, N. Stephan, L. Brehmer, Dielectric properties of zinc phthalocyanine thin films: effects of annealing in air and in $N_2$, Thin Solid Films 474 (2005) 301–305.

[12] A. Generosi, V. Rossi Albertini, G. Rossi, G. Pennesi, R. Caminiti, Energy dispersive X-ray reflectometry of the $NO_2$ interaction with ruthenium phtalocyanine films, J. Phys. Chem. B 2 (2003) 575–579.

[13] A. Generosi, B. Paci, V. Rossi Albertini, P. Perfetti, A.M. Paoletti, G. Pennesi, G. Rossi, R. Caminiti, Experimental evidence of a two steps absorption/desorption process in ruthenium phtalocyanine gas sensing films by in situ energy dispersive X-ray reflectometry, Appl. Phys. Lett. 86 (2005) 114106–114108.

[14] M. Naddaf, S. Chakane, S. Jain, S.V. Bhoraskar, A.B. Mandale, Modification of sensing properties of metallophthalocyanine by an ECR plasma, Nucl. Instrum. Methods B 194 (2002) 54–60.

[15] L.G. Parratt, Surface studies of solids by total reflection of X-rays, Phys. Rev. 95 (1954) 359–369.

[16] R. Felici, On the use of energy dispersive X-ray reflection to study the electronic density profile at surfaces and interfaces, Rigaku J. 12 (1995) 11–17.

[17] V. Rossi Albertini, B. Paci, A. Generosi, The energy dispersive X-ray reflectometry as a unique laboratory tool to investigate morphological properties of layered systems and devices, J. Phys. D: Appl. Phys. 39 (2006) 461–486.

[18] R. Caminiti, V. Rossi Albertini, Review on the kinetics of phase transitions observed by energy dispersive X-ray diffraction, Int. Rev. Phys. Chem. 18 (1999) 263–299.

[19] K. Orita, T. Morimura, T. Horiuchi, K. Matsushige, In situ energy-dispersive X-ray reflectivity measurements of structural changes in thin films for organic electroluminescent devices, Synth. Met. 91 (1997) 155–158.

[20] A. Plech, U. Klemradt, H. Metzger, J. Peisl, In situ X-ray reflectivity study of the oxidation kinetics of liquid gallium and the liquid alloy $Ga_{0.93}Hg_{0.07}$, J. Phys. Condens. Matter 10 (1998) 971–982.

[21] R. Caminiti, A. Capobianchi, P. Marovino, A.M. Paoletti, G. Pennesi, G. Rossi, Structural and morphological characterisation of ruthenium phthalocyanine films by energy dispersive X-ray diffraction and atomic force microscopy, Thin Solid Films 382 (2001) 74–80.

[22] A. Capobianchi, G. Pennesi, A.M. Paoletti, G. Rossi, R. Caminiti, C. Sadun, C. Ercolani, Ruthenium phthalocyanine and its reaction with dioxygen: synthesis, structure, magnetism, and electrical conductivity properties of the cofacially assembled ruthenoxane aggregate of formula $HO-[(Pc)RuO]_n-H$ (average $n = 11$), Inorg. Chem. 35 (1996) 4643–4648.

[23] R. Caminiti, M.P. Donzello, C. Ercolani, C. Sadun, Further structural information on the intra- and interunit contacts in dimeric ruthenium phthalocyanine, Inorg. Chem. 38 (1999) 3027–3029.

[24] A. Capobianchi, A.M. Paoletti, G. Pennesi, G. Rossi, Italian Patent No. RM 2000 A 0000 28.

[25] A. Generosi, B. Paci, V. Rossi Albertini, P. Perfetti, A.M. Paoletti, G. Pennesi, G. Rossi, R. Caminiti, Real time joint energy dispersive X-ray reflectivity and conductivity measurements upon $NO_2$ sensing $Ti(Pc)_2$ devices, Sens. Actuators B 129 (2008) 134–138.

## Biographies

**Amanda Generosi** received Laurea degree in chemistry and PhD degree in materials science from the University of Rome La Sapienza. She got a post-doctoral fellowship at the I.S.M., C.N.R., in Rome, working in collaboration with the X-ray Spectroscopy Laboratory. Her main activities cover the structural/morphological investigations of layered materials as basis for gas sensing devices and for renewable energy sources (plastic solar cells and fuel cells).

**Barbara Paci** received Laurea degree in physics, summa con laude, and PhD in physics. At present, she is a researcher at I.S.M., C.N.R. in Rome, and some of her

major research activities focus on the structural and morphological study of novel materials, films and devices for application as organic photovoltaic cells, as fuel cells, and as gas sensing. *Interests*: molecular physics, organic films for non-linear optics, amorphous solids, electronic and electrochemical devices. *Expertise*: X-ray (laboratory and synchrotron), neutron, linear and non-linear optical (pump and probe) techniques and computer simulations.

**Valerio Rossi Albertini** received Laurea degree in physics, PhD in materials science. Responsible of the "X-ray Spectroscopy Laboratory" at I.S.M., C.N.R. in Rome. *Interests*: molecular physics, liquids and amorphous solids, electronic and electrochemical devices. *Expertise*: X-ray (laboratory and synchrotron) and neutron techniques, IR spectroscopy, computer simulations and ab initio calculations.

**Renato Generosi** received "Perito diploma" with specialization in industrial electronic (electronic engineer). He is the responsible of the Electronic Laboratory at I.S.M., C.N.R. He is expert in scanning probe microscopy.

**Anna Maria Paoletti** had PhD in chemical sciences, is currently a senior scientist at the Institute of Structure of Matter of CNR in the research field of molecular materials with non-conventional properties, her work includes the study of phthalocyanine compounds material for optoelectronics and photonics.

**Giovanna Pennesi** graduated in chemistry, is currently a senior scientist at the Institute of Structure of Matter of CNR in the research field of molecular materials with non-conventional properties, her work attained mostly at the utilization and characterization of phthalocyanine compounds as thin films in optical and conductometric gas-sensors for the environmental monitoring.

**Gentilina Rossi** graduated in chemistry is a senior scientist at the Institute of Structure of Matter of CNR and leads the Group of Molecular Materials with non-conventional Properties in the same Institute; her research interests are in the field of synthesis, characterization and development of new phthalocyanine compounds useful for application in electronic or optical devices.

**Marco Fosca** received Laurea degree in chemistry from the University of Rome La Sapienza. He got a fellowship at the I.S.M., C.N.R., in Rome, working in collaboration with the X-ray Spectroscopy Laboratory. His main activity focuses on the study of gas sensing devices.

**Ruggero Caminiti** graduated in chemistry at the University of Rome. He is currently a full professor of *physical chemistry* at Rome's University "La Sapienza" (since 2001) being the responsible of the Laboratory of X-ray Diffraction. *Interests*: EDXD and EDXR, biomembrane models and disordered systems.